CORONAVIRUS

Genomic assessment of invasion dynamics of SARS-CoV-2 Omicron BA.1

Joseph L.-H. Tsui[1]*, John T. McCrone[2,3]†, Ben Lambert[4]†, Sumali Bajaj[1]†, Rhys P. D. Inward[1]†, Paolo Bosetti[5]†, Rosario Evans Pena[1]†, Houriiyah Tegally[6,7], Verity Hill[2,8], Alexander E. Zarebski[1], Thomas P. Peacock[9,10], Luyang Liu[11], Neo Wu[11], Megan Davis[12], Isaac I. Bogoch[13], Kamran Khan[12,13], Meaghan Kall[10], Nurin Iwani Binti Abdul Aziz[10], Rachel Colquhoun[2], Áine O'Toole[2], Ben Jackson[2], Abhishek Dasgupta[1,14], Eduan Wilkinson[6,7], Tulio de Oliveira[6,7], The COVID-19 Genomics UK (COG-UK) consortium¶, Thomas R. Connor[15,16,17], Nicholas J. Loman[18], Vittoria Colizza[19], Christophe Fraser[20,21], Erik Volz[22], Xiang Ji[23], Bernardo Gutierrez[1,24], Meera Chand[10], Simon Dellicour[25,26], Simon Cauchemez[5]‡, Jayna Raghwani[1,27]‡, Marc A. Suchard[28]‡, Philippe Lemey[26]‡, Andrew Rambaut[2]‡, Oliver G. Pybus[1,21,27]*‡, Moritz U. G. Kraemer[1,21]*‡

Severe acute respiratory syndrome coronavirus 2 (SARS-CoV-2) variants of concern (VOCs) now arise in the context of heterogeneous human connectivity and population immunity. Through a large-scale phylodynamic analysis of 115,622 Omicron BA.1 genomes, we identified >6,000 introductions of the antigenically distinct VOC into England and analyzed their local transmission and dispersal history. We find that six of the eight largest English Omicron lineages were already transmitting when Omicron was first reported in southern Africa (22 November 2021). Multiple datasets show that importation of Omicron continued despite subsequent restrictions on travel from southern Africa as a result of export from well-connected secondary locations. Initiation and dispersal of Omicron transmission lineages in England was a two-stage process that can be explained by models of the country's human geography and hierarchical travel network. Our results enable a comparison of the processes that drive the invasion of Omicron and other VOCs across multiple spatial scales.

Since the emergence of SARS-CoV-2 in late 2019, multiple variants of concern (VOCs) have sequentially dominated the pandemic worldwide. The Omicron VOC (Pango lineage B.1.1.529, later divided into lineages including BA.1 and BA.2) was discovered in late November 2021 through genomic surveillance in Botswana and South Africa and a traveler from South Africa in Hong Kong (*1*); it was designated a VOC by the World Health Organization on 26 November (*2*). An initial surge in Omicron cases in South Africa indicated a higher transmission rate than previous VOCs (*3*), which studies later attributed to a shorter serial interval, increased immune evasion, and greater intrinsic transmissibility (*4*–*7*). The mechanism for greater transmissibility is hypothesized to be altered tropism and higher replication in the upper respiratory tract (*8*, *9*). Together with waning levels of population immunity from previous infections and vaccination (*10*), local transmission of Omicron BA.1 was reported soon thereafter in travel hubs worldwide, including New York City and London by early December 2021, despite travel restrictions on international flights from multiple southern African countries (*11*, *12*).

Following the first confirmed case of Omicron in England on 27 November 2021 (*13*), Omicron prevalence increased rapidly across all regions of England, with Greater London prevalence peaking first in mid-December at ~6% followed by the South East region (*14*). Other metropolitan areas in North West and North East England saw similar but delayed increases in prevalence with observed peaks between early- and mid-January 2022. By January 2022, Omicron incidence had declined substantially in Greater London and other southern regions resulting in decreasing prevalence from north to south England (*15*). Rapid growth in infections during the initial emergence of Omicron in England prompted the UK government to impose interventions including a move to "Plan B" non-pharmaceutical restrictions (mandatory COVID pass for entry into certain venues, face coverings, and work-from-home guidance) on 8 December 2021 (*16*), in addition to an accelerated program of booster vaccination for all adults by mid-December 2021 (*17*). SARS-CoV-2 prevalence in England decreased later in January 2022, coincident with a falling proportion of BA.1 infections as lineage BA.2 became the dominant lineage; BA.2 was itself later replaced by lineages BA.4 and BA.5 (*18*–*20*).

Understanding and quantifying the relative contributions of the factors that determined the arrival and spatial dissemination of Omicron BA.1 in England can help inform the design of spatially targeted interventions against VOCs (*21*). We analyzed the Omicron BA.1 wave in England, using a dataset of 48,748 Omicron BA.1 genomes from England. This dataset represents ~1% of all confirmed Omicron BA.1 cases in England during the study period and is combined with aggregated and anonymized human mobility and epidemiological data from lower tier local authorities (LTLAs) in England.

International importation and Omicron BA.1 lineage dynamics

To investigate the timing of virus importations into England and the dynamics of the resulting local transmission lineages, we undertook a large-scale phylodynamic analysis of 115,622 SARS-CoV-2 Omicron genomes, sampled globally between 8 November 2021 and 31 January 2022. About 42% (n = 48,748) were sampled from England and sequenced by the COVID-19 Genomics UK (COG-UK) consortium (*22*). All available genomes [from COG-UK and the Global Initiative on Sharing All Influenza Data (GISAID) (*23*) on 12 and 9 April 2022, respectively] sampled before 28 November 2021 were included; later genomes were subsampled randomly in proportion to weekly Omicron case incidence while maintaining a ~1:1 ratio between English and non-English samples. To reduce potential bias caused by heterogeneous sequencing coverage, we performed a weighted subsampling of

[1]Department of Biology, University of Oxford, Oxford, UK. [2]Institute of Ecology and Evolution, University of Edinburgh, Edinburgh, UK. [3]Helix, San Mateo, CA 94401, USA. [4]College of Engineering, Mathematics and Physical Sciences, University of Exeter, Exeter, UK. [5]Institut Pasteur, Université Paris Cité, CNRS, Paris, France. [6]KwaZulu-Natal Research Innovation and Sequencing Platform (KRISP), Nelson R. Mandela School of Medicine, University of KwaZulu-Natal, Durban, South Africa. [7]Centre for Epidemic Response and Innovation (CERI), School for Data Science and Computational Thinking, Stellenbosch University, Stellenbosch, South Africa. [8]Department of Epidemiology of Microbial Diseases, Yale School of Public Health, New Haven, CT 06511, USA. [9]Department of Infectious Disease, Imperial College London, London, UK. [10]UK Health Security Agency, London, UK. [11]Google Research, Mountain View, CA 94043, USA. [12]BlueDot, Toronto, Canada. [13]Department of Medicine, Division of Infectious Diseases, University of Toronto, Toronto, Canada. [14]Doctoral Training Centre, University of Oxford, Oxford, UK. [15]Pathogen Genomics Unit, Public Health Wales NHS Trust, Cardiff, UK. [16]School of Biosciences, The Sir Martin Evans Building, Cardiff University, Cardiff, UK. [17]Quadram Institute, Norwich, UK. [18]Institute of Microbiology and Infection, University of Birmingham, Birmingham, UK. [19]Sorbonne Université, INSERM, Institut Pierre Louis d'Épidémiologie et de Santé Publique (IPLESP), Paris, France. [20]Big Data Institute, Li Ka Shing Centre for Health Information and Discovery, Nuffield Department of Medicine, University of Oxford, UK. [21]Pandemic Sciences Institute, University of Oxford, Oxford, UK. [22]MRC Centre of Global Infectious Disease Analysis, Jameel Institute for Disease and Emergency Analytics, Imperial College London, London, UK. [23]Department of Mathematics, Tulane University, New Orleans, LA 70118, USA. [24]School of Biological and Environmental Sciences, Universidad San Francisco de Quito USFQ, Quito, Ecuador. [25]Spatial Epidemiology Lab (SpELL), Université Libre de Bruxelles, Bruxelles, Belgium. [26]Department of Microbiology, Immunology and Transplantation, Rega Institute, KU Leuven, Leuven, Belgium. [27]Department of Pathobiology and Population Science, Royal Veterinary College, London, UK. [28]Departments of Biostatistics, Biomathematics and Human Genetics, University of California, Los Angeles, CA 90095, USA.
*Corresponding author. Email: lok.tsui@new.ox.ac.uk (J.L.H.T.); opybus@rvc.ac.uk (O.G.P.); moritz.kraemer@biology.ox.ac.uk (M.K.)
†These authors contributed equally to this work.
‡These authors contributed equally to this work.
¶Consortium members and affiliations are listed in the Supplementary Materials.

the English genomes using a previously developed procedure that accounts for variation in the number of sequences sampled per reported case at the upper tier local authority (UTLA) level (*24*) (supplementary materials).

We identified at least 6455 [95% highest posterior density (HPD): 6184 to 6722] independent importation events. Most imports from outside of England [69.9% (95% HPD: 69.0 to 70.7)] led to singletons (i.e., a single genome sampled in England associated with an importation event, which did not lead to observable local transmission in our dataset). The earliest importation is estimated between 5 and 18 November [approximated as the midpoint between the inferred times of the most recent common ancestor (MRCA) of the transmission lineage and the parent of the MRCA (PMRCA)]. Between the first introduction and mid-December 2021, we reconstruct an approximately exponential increase in the daily number of imports, before a plateau in early January 2022 (Fig. 1C). Daily importation rate may have risen between 22 November (when Omicron was first reported) and 25 November (when travel restrictions started). Increased outflows of air passengers before (and possibly in anticipation of) the imposition of travel restrictions have been reported for SARS-CoV-2 elsewhere (*25*, *26*). The importation rate appears to re-accelerate early in December, despite restrictions on incoming international travel from 11 southern African countries; imports then could have originated from BA.1 outbreaks in other countries in late November and early December 2021.

To explore this hypothesis, we calculate the estimated importation intensity (EII) of Omicron BA.1 from countries with the highest air traffic volumes to England, capturing 80% of incoming passengers. For each source location, the EII combines the weekly average COVID-19 test positivity rate, weekly relative prevalence of Omicron BA.1 genomes, and monthly number of observed air passengers traveling to England and thus represents a relative rate of importation (details and sensitivity analyses are available in supplementary materials; figs. S4 to S6). Although the earliest imports were inferred to have come mostly from South Africa, we observe a diversification in the inferred sources of BA.1 imports by late November and early December 2021 (Fig. 2A), during the period of travel restrictions (mandatory hotel quarantine) (*27*) on international travel from South Africa. We conclude that the exponential growth of BA.1 importations through mid-December is in part due to introductions from countries other than South Africa (Fig. 1B and Fig. 2), as a result of their growing Omicron epidemics and substantial air travel volumes to England (fig. S4). When travel restrictions for 11 southern African countries were first announced (Fig. 1A), BA.1 genome sequences from only four countries globally had been uploaded to GISAID (*23*). We note that our work is not designed to quantitatively assess the impact of travel restrictions on infection numbers in England.

To cross-validate the importation dynamics inferred from viral genomes and EIIs using independent data, we collated the travel history of inbound travelers who later tested positive for BA.1 following their arrivals (data generated by the UK Health Security Agency; supplementary materials). The early temporal profile of importation from these data are consistent with that inferred from both the EIIs and the phylodynamic analysis (until mid-December; Fig. 2A), with the growth of the latter being

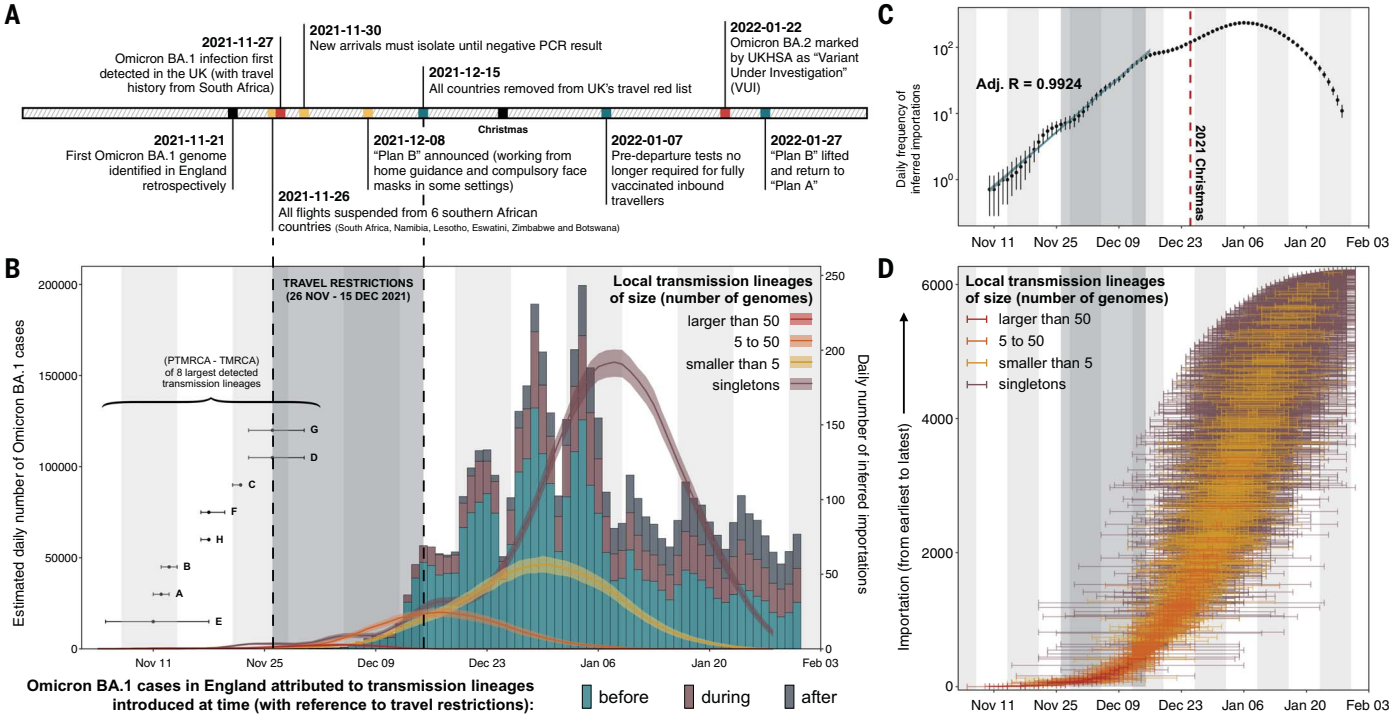

Fig. 1. Dynamics of BA.1 transmission lineages in England. (**A**) Timeline of events during the BA.1 wave in England until February 2022. (**B**) Histogram of estimated daily number of BA.1 cases, colored according to the proportion of cases attributable to transmission lineages imported at different times (shaded region shows period of travel restrictions). Curves show the estimated daily frequency of importation (7-day rolling average), colored according to the size of resulting local transmission lineages; shading denotes the associated 95% HPD. For each of the eight largest detected transmission lineages (A to H), the estimated time of importation, TMRCA (inferred time of most recent common ancestor) and TPMRCA (inferred time of parent of MRCA) (bottom left of the panel). (**C**) Daily frequency of importation (7-day rolling average; black dots) estimated from phylodynamic analysis, without stratification by size of resulting local transmission lineage; error bars denote the associated 95% HPD. Solid blue line represents an exponential model fitted to the observed 7-day rolling average values. (**D**) Distribution of TPMRCAs and TMRCAs of all 6455 detected introductions. Each horizontal line represents a single introduction event that led to a transmission lineage or singleton; the left limit indicates the TPMRCA and the right limit indicates the TMRCA (or genome sample date, for a singleton).

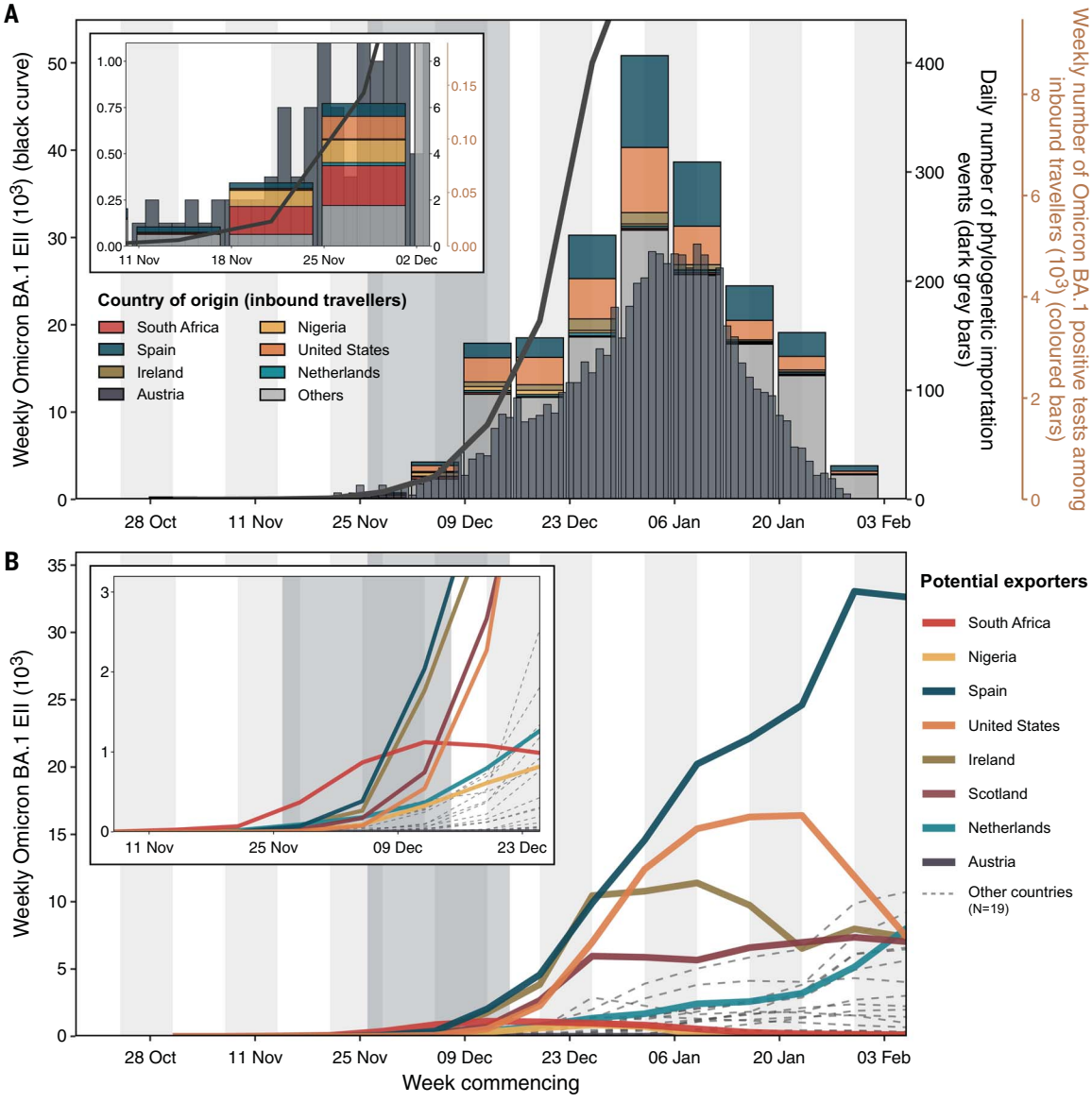

Fig. 2. Dynamics of Omicron BA.1 importation into England. (**A**) Solid curve represents the aggregated EII for 27 countries with the highest air passenger volumes to England between November 2021 and January 2022 (collectively comprising ~80% of air passengers in this period). Colored bars show the weekly number of inbound travelers who tested positive for BA.1 following arrival in the UK, extracted from travel data compiled by the UKHSA; segments are colored according to country of origin. Gray bars show the estimated daily number of importation events from phylodynamic analyses. Inset shows a magnified view of early trends. Shaded region indicates the period of travel restrictions on travel from southern African countries. (**B**) Estimated weekly number of Omicron BA.1 cases arriving in England from 27 countries with the highest air passenger volumes to England between November 2021 and January 2022 [same as those in (A)]. Thick solid lines represent weekly EII from eight countries that contribute substantially to overall EII at different times; thin gray lines represent other countries. Inset shows a magnified view of early trends. Shaded region indicates the period of travel restrictions.

slightly lagged (Fig. 2A). This observation is consistent with previous studies and is likely due to the time lag between international importation and the first local transmission event observable from genomic data (*28*). The relative frequency of genomically identified BA.1 imports among travelers from South Africa and Nigeria declined in mid-December as importation from other countries began to dominate, consistent with the EII results. Observed imports from the phylodynamic analysis also declined in January, likely due to right censoring (the last genome in our dataset was sampled on 31 January).

As with the emergence of previous VOCs in England (*28*, *29*), we find that transmission lineage sizes are overdispersed (fig. S2), with most sampled genomes belonging to a few large transmission lineages. The eight largest lineages (>700 genomes each) together comprise >60% of the English genomes in our dataset (Fig. 1B). We infer that six of these eight were imported before restrictions on travel from southern African countries were introduced (26 November), and three could have been introduced before the first epidemiological signal of Omicron [a change in S-gene target failure (SGTF), samples identified by a private lab in South Africa on 15 November; Fig. 1B]. Although aggregation of lineages as a result of unsampled genetic diversity outside England could have resulted in earlier importation estimates (*30*), this is unlikely given the enrichment of early genomes and consistency of the observed lineage size

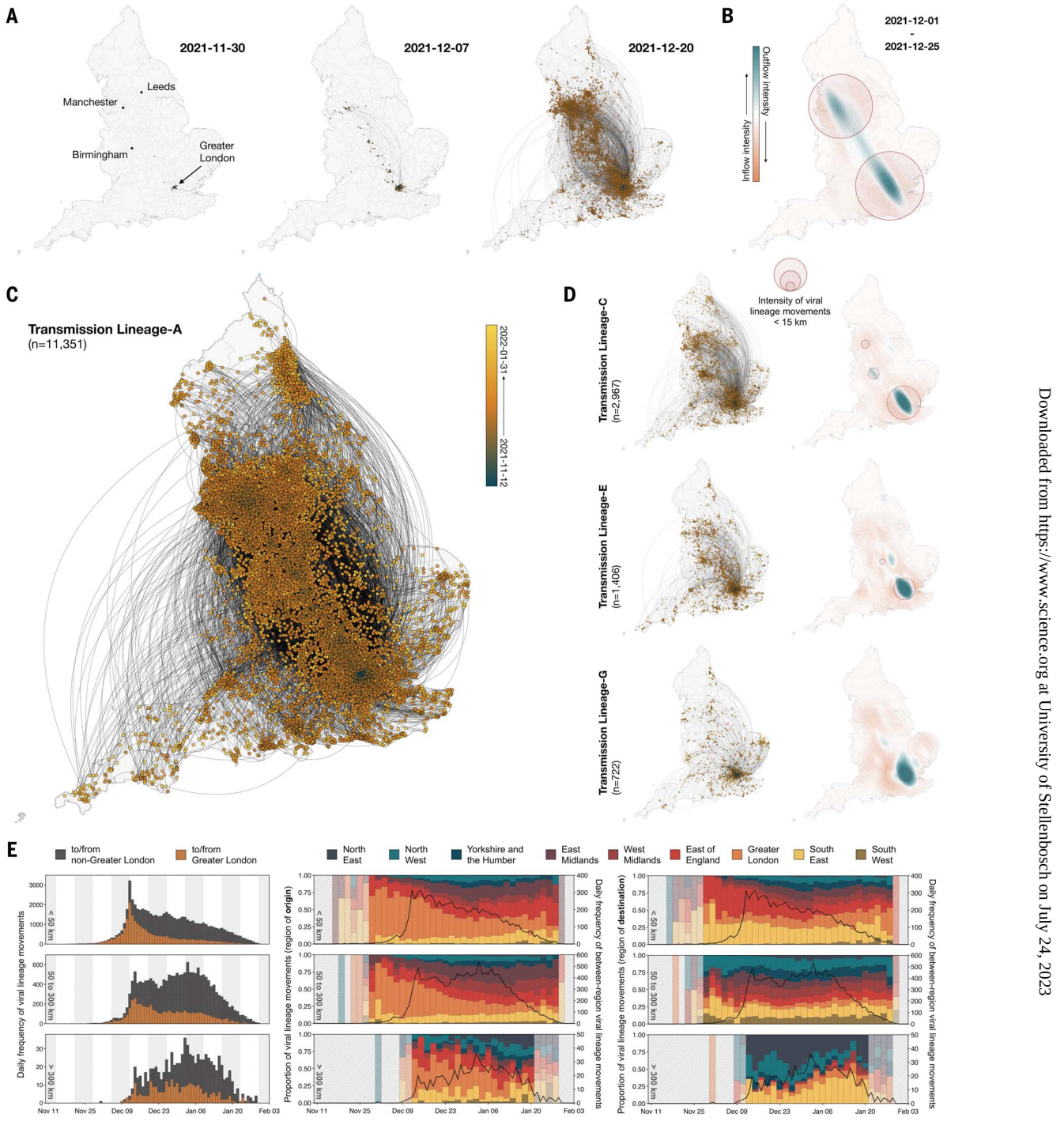

Fig. 3. Spatiotemporal dynamics of BA.1 transmission lineages in England. (**A** and **C**) Continuous phylogeographic reconstruction of the dispersal history of Transmission Lineage-A, the largest detected BA.1 transmission lineage. Nodes are colored according to inferred date of occurrence and edge curvature (anticlockwise) represents the direction of viral lineage movement. (A) shows the progress of dissemination at three specific times whereas (C) shows the complete construction. (**B**) Geographical distribution of the inflow and outflow of viral lineages within Transmission Lineage-A, from 1 December to 25 December 2021. Blue colors indicate areas with high intensity of viral lineage outflow; red colors indicate those with high intensity of inflow. Red circles indicate areas with high densities of local viral movements (distances <15 km); circle radii are proportional to that density. (**D**) Continuous phylogeographic reconstructions of Transmission Lineages-C, E, and G [as per panel (C)] with corresponding geographical distributions of viral lineage inflow and outflow [as per panel (B)]. Fig. S12 provides equivalent figures for Transmission Lineages-B, D, F, and H. (**E**) Plots in each row show viral lineage movements across different spatial scales [(top) <50 km; (middle) 50 to 300 km; (bottom) >300 km). (Left) Histograms showing the daily frequency of viral lineage movements; colors indicate whether the origin and/or destination of inferred lineage movements occurred in Greater London. (Middle/Right) Solid black lines represent the daily frequency of among-region viral lineage movements. Vertical bars indicate the proportions of viral lineage movements (aggregated at 2-day intervals); colors indicate origin/destination locations. Shaded gray areas indicate periods when there were <9 inferred viral lineage movements per day.

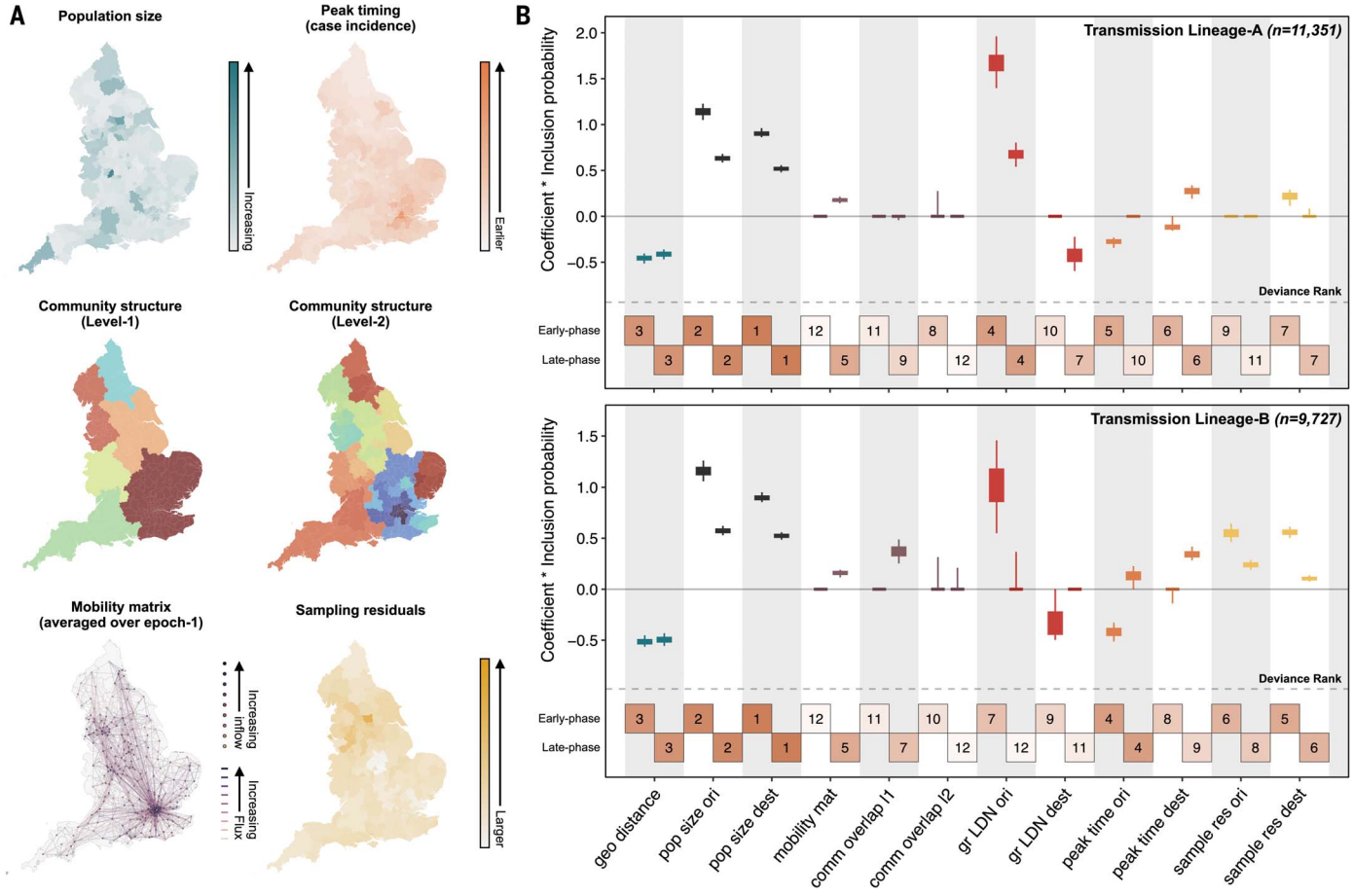

Fig. 4. Predictors of BA.1 viral lineage movements in England. (**A**) Map at LTLA level of model predictors included in the phylogeographic GLM analysis for Transmission Lineage-A. (**B**) For each predictor, the box and whiskers show the posterior distribution of the product of the log predictor coefficient and the predictor inclusion probability; the left- and right-hand values show the estimates for before and after 26 December, respectively. Top and bottom panels show estimates for Transmission Lineage-A and -B, respectively. Posterior distributions are colored according to predictor type: geographic distances (geo distance, dark blue), population sizes at origin and destination (pop size ori/dest, black), aggregated mobility matrix (mobility mat, purple), mobility-based community membership level 1 and level 2 (comm overlap l1 and l2, purple), Greater London origin and destination (gr LDN ori/dest, red), time of peak incidence at origin and destination (peak time ori/dest, orange), the residual of a regression of sample size against case count regression at origin or destination (sample res ori/dest, yellow). Boxes at the bottom of each panel are numbered and shaded to show the ranking of predictors based on their deviance measure (materials and methods), with 1 indicating the largest deviance (most important predictor) and 12 indicating the smallest (least important predictor).

distribution with that from the simulation (figs. S7 and S8). We observe a strong association between the size and time of importation of local transmission lineages, with most large transmission lineages attributed to early introductions (before mid-November) (Fig. 1B). This pattern is recapitulated by a simple mathematical model; if all lineages share the same transmission characteristics, then the date of importation is the main determinant of transmission lineage size when the epidemic in the recipient location is growing exponentially (supplementary materials; figs. S7 and S8).

We estimate that ~400 transmission lineages (including the eight largest) resulted from importation before the end of travel restrictions on 15 December (29 lineages were introduced before 26 November). Although these early imports account for only a small proportion (~6%) of the estimated number of introductions, they are responsible collectively for ~80% of estimated BA.1 infections in England by the end of January 2022.

Human mobility drives spatial expansion and heterogeneity in Omicron BA.1 growth

The rapid increase in Omicron importation in late 2021 led to the establishment of local transmission chains, initially concentrated in Greater London and neighboring LTLAs in the South West and East of England. This coincided with early increases in BA.1 prevalence in those regions, as observed from SGTF data and epidemiological prevalence surveys (*15*). To investigate further the spatiotemporal dynamics of BA.1 in England, we reconstructed the dispersal history of all identified transmission lineages (with >4 genomes) using spatially explicit phylogeographic techniques. Genomic sample sizes were highly representative of the estimated number of BA.1 cases at the UTLA level in England (figs. S9 and S10).

We observe distinct stages in the spread of BA.1 across England, with the eight largest transmission lineages sharing broadly similar patterns of spatial dispersal. Unlike other VOCs, the first detected BA.1 transmission lineages are more evenly distributed among regions, with ~20% in Greater London, ~15% in the South East, and 13% in the North West (if only introductions before December 2021 are considered, the value for Greater London is 27%). However, most early cases outside Greater London resulted in limited local spatial diffusion (Fig. 3 and figs. S11 and S12).

Initial long-distance viral lineage movements from Greater London repeatedly arrived in

multiple urban [as classified in (*30*)] conurbations in early and mid-December 2021, but local transmission was not established immediately. The fraction of viral lineage movements that were local (within-city) remained between 25 and 50% from December 2021 to January 2022 in all areas except Greater London (~90%) and Greater Manchester (~60%). This fraction grew when local mobility levels recovered after the holiday period (*31*–*34*), coinciding with the establishment of local transmission across most LTLAs in England (fig. S11). Further, cities other than Greater London acted primarily as sinks throughout the BA.1 wave, with limited backflow of long-distance viral lineages from North West England to Greater London (e.g., Transmission Lineage-A and -B; similar dynamics are seen also for South West England; Fig. 3E). We define locations as either sinks or sources according to whether there was a net flow of viral lineages into or out of the location, respectively, over the study period.

Even after the establishment of local transmission in most English LTLAs, Greater London continued to be a source of mid-to-long range viral lineage movements (Fig. 3E). This is expected given Greater London's role as a major hub in England's mobility network (similar trends were observed for the Alpha wave in 2020) (*26*). The importance of Greater London as a source of short range (<50 km) lineage movements declined through time (Fig. 3E, top left) and we observe a secondary peak in the frequency of mid-to-long range movements (>50 km) driven predominantly by lineages emanating from the Midlands and southern England (Fig. 3E, middle and right). These observations are consistent with epidemiological data showing that most areas outside of southern England experienced a BA.1 incidence peak only in the last week of December 2021 or the first week of January 2022 (fig. S13).

To assess the contribution of demographic, epidemiological, and mobility-related factors to the dissemination of BA.1 in England, we used a phylogeographic generalized linear model (GLM) to test the association of those factors with viral lineage movements among LTLAs, during two distinct periods (before 26 December 2021, and between 26 December 2021 and 31 January 2022; supplementary materials) (*32*, *33*, *35*). Using this time-inhomogeneous model we find evidence for a dynamic spatial transmission process, with the estimated effect size and relative importance of most predictors varying over time (Fig. 4B; ranking of predictors based on their deviance measure are shown in boxes). During the earlier "expansion" period of lineage dissemination, we observe strong support for the gravity model predictors (a spatial interaction model in which travel intensity between pairs of locations increases with origin and destination population sizes but decreases with distance). Consistent with results from continuous phylogeography (Fig. 3), this early period is characterized by directional viral dissemination; lineage movements tend to originate from Greater London (Fig. 4B) and this is particularly pronounced for smaller transmission lineages (Fig. 3 and fig. S12). For LTLAs with earlier times of peak incidence, we also find greater outflow of virus lineages during the expansion period (in three of four analyses) and a lower inflow of viral lineages during the post-expansion period (in four of four analyses; Fig. 4 and fig. S14). These results reflect the network-driven nature of Omicron's geographic spread, with variation in the timing of peak incidence reflecting varying degrees of connection to locations where frequent importation seeded early transmission chains (*36*).

The human mobility predictor is supported consistently only in the post-expansion phase (Fig. 4B), after local transmission has been established in most LTLAs. This reflects a transition from unidirectional long-distance movements to more homogeneous local dissemination. Conversely, support for the gravity model predictors decreased over time (Fig. 4B), consistent with the notion that the gravity model better predicts city-to-city movement and poorly describes diffusion-like mobility over short distances in urban areas (*37*). Importantly, the phylogeographic GLM results are consistent among the transmission lineages analyzed (Fig. 4B), and when a simpler time-homogenous model is used (fig. S15). These findings corroborate our continuous phylogeography analyses (Fig. 3) and epidemiological studies showing strong local spatial structure of the BA.1 wave (*14*, *15*). We also explored whether booster vaccine uptake (per capita at the LTLA level) is supported as a predictor under a time-inhomogeneous model, but found no significant support (supplementary materials), possibly a result of collinearity of this factor with other predictors or limited spatial heterogeneity in vaccine uptake.

Discussion

We find that most infections during the Omicron BA.1 wave in England can be traced back to a small number of introductions, which likely arrived before or during travel restrictions on incoming passengers from southern Africa. Although the rate of importation continued to increase after mid-December (Fig. 1C), the largest English transmission lineages tended to be those introduced earlier (Fig. 1D). These results augment previous investigations of VOCs in England and elsewhere (*28*, *38*), highlighting that international travel restrictions can have limited impacts if applied after local exponential growth is established and in the absence of local control measures. Our analyses indicate that epidemics of BA.1 in multiple locations outside the country where BA.1 was first detected contributed substantially to the growth of BA.1 importation into England in December 2021 (*39*). The impact of targeted travel restrictions may thus be constrained by the existence of multiple pathways between any two countries in the global aviation network, and such pathways often traverse highly connected locations with large travel volumes that can act as secondary sources of early importation (*36*). UK travel restrictions were intended to delay the expansion of BA.1 locally while offering additional vaccinations to at-risk individuals. However, Omicron had likely already spread internationally by the time it was detected in late November 2021, allowing the establishment of secondary locations of exportation (*39*, *40*). Therefore, any proposed global systems that aim to rapidly detect and respond to new VOCs (and emerging infectious diseases in general) should be designed around the connection structure of human mobility networks. Despite this, there are likely to be scenarios under which travel restrictions can help control, contain, or delay the spread of emerging infections (*41*, *42*); considerable additional theoretical and empirical work is needed to improve and inform rapid decision-making regarding travel during public health emergencies.

Our two phylogeographic analyses (Figs. 3 and 4) jointly show how Omicron BA.1 disseminated rapidly across England, with Greater London central to its initial dissemination. Early viral movements outside of Greater London were dominated by medium-to-long-distance travel from there; local transmission in recipient locations was observed later, coinciding with an increase in human mobility after the winter holidays (fig. S18). The epidemic is revealed to be a network-driven phenomenon with an initial expansion phase that is well described by a gravity model, followed by a period of sustained local transmission propagated by short-distance movement (*36*).

With this study, we can now compare the transmission histories of three VOC waves in England [Alpha (*26*), Delta (*29*), and Omicron] and contrast factors that influenced their dispersals. First, Omicron and Delta were introduced through international importation, whereas Alpha appeared to have originated in England (*43*). For both Omicron and Delta, early introductions from their presumed location of origin were followed by growth in importation intensity from secondary locations. While early Delta transmission clusters were observed mainly in North West England, early Omicron infections were found mostly in Greater London (*15*, *18*). Second, different NPIs and restrictions on within-country travel were implemented during the VOC waves. Although Delta arrived when NPIs in England were being relaxed, its initial spread was delayed because of lower mobility levels following a national lockdown (*29*). By contrast, Omicron was introduced when mobility had largely recovered to prepandemic levels (fig. S18).

Alpha was observed to rapidly expand from its proposed origin in southeast England—likely attributable in part to holiday travels (*26*)—and was subsequently brought under control when local mobility decreased after the introduction of NPIs (*26*). Third, the dissemination of each VOC is likely to be differentially affected by spatial variation in population immunity. Such variation was likely limited during Delta's emergence as a result of high population levels of vaccination and previous infection and also during Omicron's emergence due to the antigenic novelty of BA.1 (*9*, *44*, *45*). By contrast, initial growth rates of Alpha in England were found to be affected by local variation in previous attack rates (*26*). These findings highlight two key questions for future work: how do spatiotemporal interactions between importation and local transmission shape the spread of a VOC, and how can we efficiently evaluate the interplay of factors that drive the dissemination of new VOCs within a country?

We interpret our phylodynamic results in the context of several limitations. First, as discussed previously (*28*), the inferred number of importation events underestimates the true number of independent introductions due to incomplete sampling and uneven sequencing coverage worldwide (*46*). Nevertheless, we were able to cross-validate our phylodynamic results using independent epidemiological data (figs. S7 and S8). Second, to maintain computational tractability and remove potential sampling bias, we subsampled all available English Omicron genomes, accounting for geographical variations in sequencing coverage and prevalence. However, even after this subsampling, the spatial and temporal sampling was not perfectly representational (Fig. 4A and fig. S9). This could be due to spatial variation in case reporting rate or because the maximum sequencing capacity was exceeded in locations with high incidence. Third, our phylogeographic GLM analysis, which explores the association of factors with virus lineage movement, should be interpreted in light of potential biases in the mobility data. For example, mobility in sparsely populated locations may be poorly captured as a result of censoring to protect user anonymity, and the degree to which smartphone data are representative of the whole population is affected by variation in smartphone use among locations. Work is ongoing to assess how human mobility data can be best applied to the prediction and description of infectious disease invasion dynamics (*47*, *48*).

Omicron BA.1 was replaced by lineage BA.2 in February 2022 and later by lineage BA.5 in June 2022 (*18*, *19*). Although the public health emergency of international concern has ended (*49*) and the public health burden of COVID-19 has lessened as a result of reduced average disease severity and increased population immunity, the continued antigenic evolution of SARS-CoV-2 means that future VOCs of unknown virulence remain possible. One priority in preparing for the next VOC or novel pathogen emergence is to develop and implement robust pipelines for large-scale genomic and epidemiological analyses supported by unified data infrastructures (*50*, *51*) a challenging task that will be realized only through close coordination of public health efforts worldwide.

REFERENCES AND NOTES

1. R. Viana *et al*., *Nature* **603**, 679–686 (2022).
2. World Health Organization, Classification of Omicron (B.1.1.529): SARS-CoV-2 Variant of Concern (WHO, 2021); https://www.who.int/news-room/statements/26-11-2021-classification-of-omicron-(b.1.1.529)-sars-cov-2-variant-of-concern.
3. J. R. C. Pulliam *et al*., *Science* **376**, eabn4947 (2022).
4. A. Rössler, L. Riepler, D. Bante, D. von Laer, J. Kimpel, *N. Engl. J. Med.* **386**, 698–700 (2022).
5. F. P. Lyngse *et al*., *Nat. Commun.* **13**, 5573 (2022).
6. J. A. Backer *et al*., *Euro Surveill.* **27**, 2200042 (2022).
7. UK Health Security Agency, SARS-CoV-2 variants of concern and variants under investigation in England (Technical briefing 36, 2022); https://assets.publishing.service.gov.uk/government/uploads/system/uploads/attachment_data/file/1056487/Technical-Briefing-36-22.02.22.pdf
8. K. P. Y. Hui *et al*., *Nature* **603**, 715–720 (2022).
9. T. P. Peacock *et al*., The altered entry pathway and antigenic distance of the SARS-CoV-2 Omicron variant map to separate domains of spike protein. biorxiv 2021.12.31.474653 [Preprint] (2022).
10. S. Cele *et al*., *Nature* **602**, 654–656 (2022).
11. S. Mallapaty, *Nature* **600**, 199 (2021).
12. Prime Minister's Office, Prime Minister sets out new measures as Omicron variant identified in UK: 27 November 2021 (GOV.UK Press Release, 2021; https://www.gov.uk/government/news/prime-minister-sets-out-new-measures-as-omicron-variant-identified-in-uk-27-november-2021.
13. UK Health Security Agency, COVID-19 variants identified in the UK – latest updates. (GOV.UK, 2021); https://www.gov.uk/government/news/covid-19-variants-identified-in-the-uk-latest-updates.
14. P. Elliott *et al*., *Science* **375**, 1406–1411 (2022).
15. P. Elliott *et al*., *Science* **376**, eabq4411 (2022).
16. Prime Minister's Office, Prime Minister confirms move to Plan B in England. (GOV.UK, 2021); https://www.gov.uk/government/news/prime-minister-confirms-move-to-plan-b-in-england.
17. National Health Service, NHS sets out next steps to accelerate COVID-19 booster rollout. (NHS, 2021); https://www.england.nhs.uk/2021/12/nhs-sets-out-next-steps-to-accelerate-covid-19-booster-rollout/.
18. P. Elliott *et al*., Post-peak dynamics of a national Omicron SARS-CoV-2 epidemic during January 2022. medRxiv 2022.02.03.22270365 [Preprint] (2022).
19. M. Chadeau-Hyam *et al*., *Lancet Regional Health* **21**, 100462 (2022).
20. T. P. Peacock, SARS-CoV-2 evolution, post-Omicron. (Virological, 2022); https://virological.org/t/sars-cov-2-evolution-post-omicron/911.
21. S. Chang, D. Vrabac, J. Leskovec, J. Ugander, Estimating Geographic Spillover Effects of COVID-19 Policies From Large-Scale Mobility Networks. arXiv:2212.06224 [cs.CY] (2022).
22. The COVID-19 Genomics UK (COG-UK) consortium, *Lancet Microbe* **1**, e99–e100 (2020).
23. Y. Shu, J. McCauley, *Euro Surveill.* **22**, 30494 (2017).
24. robj411, robj411/sequencing_coverage: for B.1.1.7 phylodynamic analysis, Version v1.0, Zenodo (2021); https://zenodo.org/record/4599180.
25. M. U. G. Kraemer *et al*., *Science* **368**, 493–497 (2020).
26. M. U. G. Kraemer *et al*., *Science* **373**, 889–895 (2021).
27. Department of Health and Social Care, 6 African countries added to red list to protect public health as UK designates new variant under investigation. (GOV.UK, 2021); https://www.gov.uk/government/news/six-african-countries-added-to-red-list-to-protect-public-health-as-uk-designates-new-variant-under-investigation.
28. L. du Plessis *et al*., *Science* **371**, 708–712 (2021).
29. J. T. McCrone *et al*., *Nature* **610**, 154–160 (2022).
30. Office for National Statistics, 2011 rural/urban classification. (ONS, 2016); https://www.ons.gov.uk/methodology/geography/geographicalproducts/ruralurbanclassifications/2011ruralurbanclassification.
31. V. Charu *et al*., *PLOS Comput. Biol.* **13**, e1005382 (2017).
32. M. U. G. Kraemer, N. R. Faria, R. C. Reiner Jr., *Lancet Infect. Dis.* **17**, P330–338, (2017).
33. M. U. G. Kraemer *et al*., *Sci. Rep.* **9**, 5151 (2019).
34. B. Finkenstädt, B. Grenfell, *Proc. R. Soc. B* **265**, 211–220 (1998).
35. P. Nouvellet *et al*., *Nat. Commun.* **2**, 1090 (2021).
36. D. Brockmann, D. Helbing, *Science* **342**, 1337–1342 (2013).
37. M. U. G. Kraemer *et al*., *Lancet Infect. Dis.* **17**, 330–338 (2017).
38. C. L. Murall *et al*., *Genome Med.* **13**, 169 (2021).
39. H. Tegally *et al*., *Cell* 2023.06.001 (2023).
40. T. S. Brett, P. Rohani, *PNAS* Nexus. **1**, pgac159 (2022).
41. N. M. Ferguson *et al*., *Nature* **437**, 209–214 (2005).
42. C. Fraser, S. Riley, R. M. Anderson, N. M. Ferguson, *Proc. Natl. Acad. Sci. U.S.A.* **101**, 6146–6151 (2004).
43. V. Hill *et al*., *Virus Evol.* **8**, veac080 (2022).
44. B. J. Willett *et al*., *Nat. Microbiol.* **7**, 1161–1179 (2022).
45. C. Stein *et al*., *Lancet* **401**, 833–842 (2023).
46. A. F. Brito *et al*., *Nat. Commun.* **13**, 7003 (2022).
47. J. Wardle, S. Bhatia, M. U. G. Kraemer, P. Nouvellet, A. Cori, *Epidemics* **42**, 100666 (2023).
48. D. T. Citron *et al*., *Proc. Natl. Acad. Sci. U.S.A.* **118**, e2007488118 (2021).
49. World Health Organization, Statement on the fifteenth meeting of the International Health Regulations (2005) Emergency Committee regarding the coronavirus disease (COVID-19) pandemic (WHO, 2005); https://www.who.int/news/item/05-05-2023-statement-on-the-fifteenth-meeting-of-the-international-health-regulations-(2005)-emergency-committee-regarding-the-coronavirus-disease-(covid-19)-pandemic.
50. V. MooChy, O. Morgan, C. Ihekweazu, S. Swaminathan, *Nature* **611**, 449 (2022).
51. V. Hill, C. Ruis, S. Bajaj, O. G. Pybus, M. U. G. Kraemer, *Trends Parasitol.* **37**, 1038–1049 (2021).
52. joetsui1994, M. Kraemer, Joetsui1994/omicron-BA.1-invasion-dynamics: 12 may, 2023 - v1.0, Zenodo (2023); https://zenodo.org/record/7928698.

ACKNOWLEDGMENTS

We acknowledge the UK Health Security Agency, members of the COG-UK consortium, NHS labs and GISAID contributors (acknowledgment table of genomes used is provided on our GitHub repository) for sharing genomic data. **Funding:** COG-UK is supported by funding from UK Medical Research Council (MRC), National Institute of Health Research (NIHR; grant MC_PC_19027), and Genome Research Limited operating as Wellcome Sanger Institute. The authors acknowledge use of data generated through the COVID-19 Genomics Programme funded by the UK Department of Health & Social Care. M.U.G.K. acknowledges funding from The Rockefeller Foundation, Google.org, the Oxford Martin School Pandemic Genomics programme (also O.G.P., A.E.Z. and B.G.), European Union Horizon 2020 project MOOD (#874850) (also V.C., R.I., S.D., and P.L.), The John Fell Fund, a Branco Weiss Fellowship and Wellcome Trust grants 225288/Z/22/Z and 226052/Z/22/Z. V.H. was supported by UK BBSRC grant BB/M010996/1, J.T.M, R.C., N.L., P.L., M.A.S, and A.R. by Wellcome Trust Collaborators Award 206298/Z/17/Z. S.D. is supported by F.R.S.-FNRS (Belgium) grant F.4515.22 and FWO (Belgium) grant G098321N. P.L., M.A.S, and A.R. are supported by ERC grant 725422. AR acknowledges the support of The Bill & Melinda Gates Foundation grant OPP1175094. J.L.H.T. is supported by a Yeotown Scholarship from New College, University of Oxford. S.B. is supported by a Clarendon Scholarship, University of Oxford and NERC DTP (grant NE/S007474/1). T.P.P. is supported by the G2P-UK National Virology Consortium funded by the MRC (MR/W005611/1). I.I.B. is supported by a grant from the Canadian Institutes for Health Research (02179-000). J.R. is supported by the UKRI GCRF One Health Poultry Hub (grant B/S011269/1), one of 12 interdisciplinary research hubs funded under the UK government's Grand Challenge Research Fund Interdisciplinary Research Hub initiative (also supports O.G.P). E.V. acknowledges support from the Wellcome Trust (#220885/Z/20/Z). M.A.S. was supported by US NIH grants R01 AI153044 and R01 AI162611. M.A.S. and X.J. acknowledge support from NVIDIA Corporation and Advanced Micro Devices, Inc. with the donation of parallel computing resources. S.C. acknowledges Labex IBEID (grant ANR-10-LABX-62-IBEID), EU Horizon 2020 projects VEO (874735) and RECOVER (101003589), AXARF, Groupama, EMERGEN (ANRS0151) and

INCEPTION (PIA/ANR-16-CONV-0005). V.C. acknowledges funding from the European Union Horizon 2020 projects RECOVER (101003589), Horizon Europe project ESCAPE (101095619), ANRS-MIE project EMERGEN (ANRS0151). E.W., H.T., and T.d.O. are supported in part by grants from the Rockefeller Foundation (HTH 017), Abbott Pandemic Defense Coalition (APDC), the African Society for Laboratory Medicine the National Institute of Health USA (U01 AI151698) for the United World Antivirus Research Network (UWARN) and the INFORM Africa project through IHVN (U54 TW012041), the SAMRC South African mRNA Vaccine Consortium (SAMVAC), CoVICIS (101046041). The views expressed are those of the authors and not necessarily those of the Department of Health and Social Care, UKHSA, European Commission, or any other funder. **Author contributions:** J.L.H.T., O.G.P., M.U.G.K. conceived and planned the research. J.L.H.T., S.B., B.L., V.H., J.T.M., P.B., R.E.P., J.R., P.L., and S.D. analyzed the data. A.E.Z., T.P.P., B.J., R.C., E.V., M.K., N.I.B.A.A., A.O'T., A.D., J.T.M., B.L., S.C., S.D., J.R., X.J., M.A.S., M.U.G.K., O.G.P., and A.R. advised on methodologies. I.I.B., K.K., and M.D. contributed international flight data. J.L.H.T., O.G.P., and M.U.G.K. wrote the initial manuscript draft. All authors edited, read, and approved the manuscript. **Competing interests:** K.K. is the founder of BlueDot, a social enterprise that develops digital technologies for public health. M.D. is employed at BlueDot. All other authors declare no competing interests. L.L. and N.W. are employed by Google and own equity in Alphabet. J.T.M is employed by Helix. O.G.P., A.R., and A.O'T. have undertaken consulting relating to the genetic diversity and classification of SARS-COV-2 lineages. **Data and materials availability:** UK genomes were generated by (COG-UK, https://www.cogconsortium.uk/). Data linking COG-IDs to location have been removed to protect privacy, please visit https://www.cogconsortium.uk/contact/ for information on accessing consortium-only data. The Google COVID-19 Aggregated Mobility Research Dataset used for this study is available with permission from Google LLC, requests should be addressed to Aaron Schneider at aaronschneider@google.com. Code and data are available (*52*).

SUPPLEMENTARY MATERIALS

Submitted 12 January 2023; accepted 15 June 2023
10.1126/science.adg6605

Genomic assessment of invasion dynamics of SARS-CoV-2 Omicron BA.1

Joseph L.-H. Tsui, John T. McCrone, Ben Lambert, Sumali Bajaj, Rhys P. D. Inward, Paolo Bosetti, Rosario Evans Pena, Houriiyah Tegally, Verity Hill, Alexander E. Zarebski, Thomas P. Peacock, Luyang Liu, Neo Wu, Megan Davis, Isaac I. Bogoch, Kamran Khan, Meaghan Kall, Nurin Iwani Binti Abdul Aziz, Rachel Colquhoun, ine OToole, Ben Jackson, Abhishek Dasgupta, Eduan Wilkinson, Tulio de Oliveira, The COVID-19 Genomics UK (COG-UK) consortium, Thomas R. Connor, Nicholas J. Loman, Vittoria Colizza, Christophe Fraser, Erik Volz, Xiang Ji, Bernardo Gutierrez, Meera Chand, Simon Dellicour, Simon Cauchemez, Jayna Raghwani, Marc A. Suchard, Philippe Lemey, Andrew Rambaut, Oliver G. Pybus, and Moritz U. G. Kraemer

Science, **381** (6655), .
DOI: 10.1126/science.adg6605

Editor's summary

The severe acute respiratory syndrome coronavirus 2 pandemic changed character with the emergence of the Omicron lineage in South Africa in 2021. This lineage showed elevated transmissibility and increased immune evasion. Tsui *et al*. traced the history of the introduction of this variant in the United Kingdom, where exceptionally comprehensive genetic sampling regimes were established. The authors found that the virus had been introduced undetected into England between 5 and 18 November 2021, and South African scientists alerted the World Health Organization on 22 November 2021. However, by the time the UK government had responded, the variant had already spread between UK cities and globally. Therefore, the subsequent travel restrictions placed on southern Africa were futile. —Caroline Ash